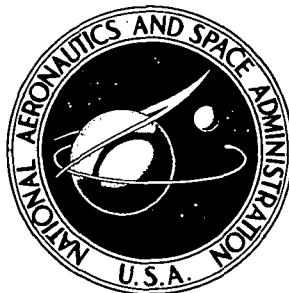


**NASA TECHNICAL  
MEMORANDUM**



**NASA TM X-3492**

**NASA TM X-3492**

**ANALYSIS OF SEPARATION  
OF THE SPACE SHUTTLE ORBITER  
FROM A LARGE TRANSPORT AIRPLANE**

*Alan W. Wilbite*

*Langley Research Center*

*Hampton, Va. 23665*

1. Report No. NASA TM X-3492	2. Government Accession No.	3. Recipient's Catalog No.	
4. Title and Subtitle ANALYSIS OF SEPARATION OF THE SPACE SHUTTLE ORBITER FROM A LARGE TRANSPORT AIRPLANE		5. Report Date June 1977	6. Performing Organization Code
		8. Performing Organization Report No. L-11074	
7. Author(s) Alan W. Wilhite	10. Work Unit No. 506-26-10-08		11. Contract or Grant No.
9. Performing Organization Name and Address NASA Langley Research Center Hampton, VA 23665		13. Type of Report and Period Covered Technical Memorandum	
		14. Sponsoring Agency Code	
12. Sponsoring Agency Name and Address National Aeronautics and Space Administration Washington, DC 20546		15. Supplementary Notes	
16. Abstract <p>An investigation has been conducted to determine the feasibility of safely separating the space shuttle orbiter (140A/B) from the top of a large carrier vehicle (the C-5 airplane) at subsonic speeds. The longitudinal equations of motion for both vehicles were numerically integrated using a digital computer program which incorporates experimentally derived interference aerodynamic data to analyze the separation maneuver for various initial conditions. From this study, separation of the space shuttle orbiter from a carrier vehicle was shown to be feasible for a range of dynamic-pressure and flight-path-angle conditions. By using an autopilot, the vehicle attitudes were held constant which ensured separation. Carrier-vehicle engine thrust, landing gear, and spoilers provide some flexibility in the separation maneuver.</p>			
17. Key Words (Suggested by Author(s)) Separation trajectory Space shuttle orbiter Active controls		18. Distribution Statement Unclassified - Unlimited  Subject Category 08	
19. Security Classif. (of this report) Unclassified	20. Security Classif. (of this page) Unclassified	21. No. of Pages 21	22. Price* \$3.50

# ANALYSIS OF SEPARATION OF THE SPACE SHUTTLE ORBITER

## FROM A LARGE TRANSPORT AIRPLANE

Alan W. Wilhite  
Langley Research Center

### SUMMARY

The feasibility of separating the space shuttle orbiter from a large transport carrier vehicle at subsonic speeds has been determined. To analyze the separation maneuver, the longitudinal equations of motion for both vehicles were integrated by a digital computer program which uses interference aerodynamic data to compute the forces and moments acting on the vehicles. The effects of active controls, dynamic pressure, and flight-path angle on the separation maneuver were determined. Also, to maximize horizontal separation distance, various high-drag configurations of the carrier vehicle were studied.

The results of this study indicate that the separation of the space shuttle orbiter from a carrier vehicle is feasible for a range of dynamic-pressure and flight-path-angle conditions. Active controls are required to hold vehicle attitudes which ensure separation. A maximum horizontal separation distance was achieved with carrier-vehicle inboard engines in reverse thrust, outboard engines in idle thrust, and spoilers and landing gear deployed.

### INTRODUCTION

Prior to 1974, the National Aeronautics and Space Administration (NASA) investigated various ways to transport the space shuttle orbiter for both ferry and flight-test missions. One study conducted by the Lockheed-Georgia Company involved the C-5 Piggyback concept in which the C-5 airplane is used both as a ferry for the orbiter and as a launch platform during orbiter approach and landing tests. Wind-tunnel data obtained during that study are the basis for this investigation.

In order to perform the approach and landing tests, the orbiter must be safely separated from the large carrier airplane. This type of separation differs from other separation problems such as the separation of an external store from a parent vehicle, in which only the aerodynamic characteristics of the smaller external store are noticeably disturbed from nominal flight conditions. The separation of two vehicles of similar size can be mutually disturbing to the aerodynamic characteristics of both vehicles; therefore, it is necessary to analyze the motions of both vehicles by separation analyses. In reference 1 this type of problem is described, and a digital computer program, which uses the disturbed aerodynamics of each vehicle to numerically integrate the equations of motion, is discussed.

The purpose of this paper is to present the results of an analysis related to the separation of the 140A/B orbiter from the Lockheed C-5 airplane. The aerodynamic data used in this analysis (ref. 2), obtained in the Lockheed-Georgia Company Low-Speed Wind Tunnel, were measured with the vehicles in proximity. Only a longitudinal analysis was conducted since insufficient lateral-directional proximity data were obtained. The parameters investigated in this paper include dynamic pressure, flight-path angle, and orbiter incidence angle relative to the carrier vehicle. Also studied were the effects of active orbiter and carrier-vehicle controls on the separation maneuver.

#### SYMBOLS AND ABBREVIATIONS

$\bar{c}$	mean aerodynamic chord, m
$C_D$	drag coefficient, Drag/ $q_\infty S$
$C_L$	lift coefficient, Lift/ $q_\infty S$
$C_m$	pitching-moment coefficient, Pitching moment/ $q_\infty S \bar{c}$
$C_{m\dot{\theta}}$	damping in pitch, $\partial C_m / \partial (\dot{\theta} \bar{c} / 2V)$ , rad <sup>-1</sup>
$d$	horizontal separation distance, m (see fig. 10)
$g$	gravitational acceleration, m/sec <sup>2</sup>
$h$	altitude, m
$I_y$	mass moment of inertia about pitch axis, kg-m <sup>2</sup>
$K_1, K_2$	autopilot gains
$l$	reference length, m
$M$	Mach number
$m$	mass, kg
$\bar{n}$	normal load factor, Normal load/ $g$
$\Delta \bar{n}$	difference between value of normal load factor for orbiter and value for carrier vehicle, $\bar{n}_O - \bar{n}_C$
$q_\infty$	dynamic pressure, Pa
$S$	reference wing area, m <sup>2</sup>
$t$	time, sec
$V$	velocity, m/sec

$X_{cg}, Z_{cg}$  center of gravity coordinates, m  
 $\Delta X, \Delta Z$  separation position variables, m (see fig. 2)  
 $\alpha$  angle of attack, deg  
 $\alpha_{com}$  commanded angle of attack for autopilot, deg  
 $\alpha_i$  orbiter incidence angle relative to the carrier vehicle,  $\alpha_o - \alpha_c$ , deg  
 $\gamma$  flight-path angle, deg  
 $\delta$  control deflection, deg  
 $\delta_e$  deflection angle of C-5 elevator or orbiter elevon, positive with trailing edge down, deg  
 $\dot{\delta}_{e,max}$  maximum control deflection rate,  $\partial\delta_e/\partial t$ , deg/sec  
 $\theta$  pitch angle, deg  
 $\dot{\theta}$  pitch rate,  $\partial\theta/\partial t$ , deg/sec  
 $\dot{\theta}_{com}$  commanded pitch rate for autopilot, deg/sec

Subscripts:

c carrier vehicle  
 o orbiter

Abbreviations:

c.g. center of gravity  
 WL water line

### DETAILS OF CONFIGURATIONS

Sketches of the 140A/B space shuttle orbiter and C-5 carrier airplane in the mated ferry configuration are shown in figure 1. As illustrated, the carrier airplane is modified with a three-point support/release mechanism to accommodate the orbiter, and the space shuttle orbiter (ref. 3) was modified with a tail fairing to reduce base drag of the orbiter and flutter and buffeting on the carrier airplane tail. Structural details of the mated configuration are presented in reference 2. In the ferry position, the lower surface of the orbiter is approximately 2 m above the top of the carrier vehicle, and its horizontal axis is inclined at  $0.5^\circ$ . In the launch configuration, the orbiter rotates on its rear mounting points until the horizontal axis is inclined at the desired incidence angle. This rotation is attained by elevating the forward mounting

point. To achieve separation, the orbiter is released from all three mounting points simultaneously, and an aerodynamic separation is performed.

## METHOD OF ANALYSIS

In reference 1, the analysis of the longitudinal separation of two vehicles in proximity to each other is described. Although the equations of motion are identical to a single body trajectory analysis, the computer program described in reference 1 uses a four-parameter look-up routine to determine the aerodynamic coefficients of each vehicle at each relative position and angular orientation during the trajectory. A pictorial representation of the actual separation motions of the vehicles is also presented in reference 1. This program was expanded to analyze both preseparation and separation maneuvers and also the effects of aerodynamic controls. For the preseparation maneuver, the forces, moments, and mass properties of the two vehicles were combined to represent the mated vehicle. The computer program simply integrated the equations of motion for two vehicles having characteristics identical to those of the mated vehicle. At launch, the vehicle characteristics were changed to represent the two separate vehicles with the initial launch conditions equal to the final prelaunch conditions.

Because insufficient lateral-directional proximity aerodynamic data were obtained during the wind-tunnel tests conducted by Lockheed-Georgia Company (ref. 2), only a longitudinal analysis was made in the present study. Table I indicates the angular orientation and relative positions (shown geometrically in fig. 2) of the vehicles for which the longitudinal aerodynamic data were obtained. For each position and incidence angle  $\alpha_i$ ,  $\alpha_c$  was varied from  $-8^\circ$  to  $15^\circ$ . The proximity aerodynamic data obtained for the test orbiter were corrected to reflect the characteristics of a current orbiter configuration (ref. 3) by taking the difference between the proximity and interference-free characteristics and adding the result to the interference-free characteristics of the test orbiter. This correction resulted in the study characteristics for the 140A/B orbiter. The wind-tunnel drag data for both the orbiter and the carrier airplane were extrapolated to flight conditions by corrections to account for the difference in skin friction. Since the wind-tunnel data were obtained at a Mach number of 0.20, it was assumed that compressibility effects were negligible for the Mach number range of interest.

The separation computer numerically integrates the equations of motion for both vehicles. The values of the aerodynamic coefficients  $C_L$ ,  $C_D$ , and  $C_m$  are obtained by a linear interpolation between discrete points of the four-parameter ( $\alpha_c$ ,  $\alpha_i$ ,  $\Delta X$ , and  $\Delta Z$ ) wind-tunnel aerodynamic data matrix at each integration step. Since control effectiveness only changed slightly for both vehicles from interference-free values to proximity values, the proximity control-effectiveness values shown in table II were used in the analysis and were assumed to be constant during the separation maneuver. The pitch dynamic-damping derivatives were also assumed to be constant during the separation maneuver and equal to the interference-free values. Reference 4 indicates that this assumption is valid with the vehicles oscillating in phase with each other during separation. Since the elapsed time from release to separation or collision

is on the order of 6 sec or less, the mass of each vehicle and the thrust of the carrier airplane were assumed to remain unchanged during the maneuver.

For most separation trajectory calculations, a simple attitude-hold autopilot was used for each vehicle to command angle of attack and to maintain pitch rate at zero. The autopilot was simulated by a rate and displacement control system represented by

$$\delta_e = K_1(\dot{\theta} - \dot{\theta}_{com}) + K_2(\alpha - \alpha_{com}) \quad (1)$$

where  $\dot{\theta}$  is the pitch rate,  $\alpha$  is the angle of attack, and  $K_1$  and  $K_2$  are control gains. The term  $\delta_e$  represents the angular deflection of either the elevator of the carrier vehicle or the elevon of the orbiter.

The mated-vehicle flight envelope is presented in figure 3 for three different combined mass and incidence angle conditions. The boundaries were calculated by use of the mated-vehicle aerodynamics, and they represent a service ceiling for a static rate of climb of 30 m/sec. Based on this envelope, a baseline Mach number of 0.525 and an altitude of 6.1 km were selected for the initial conditions for the separation analysis. The aerodynamic parameters and vehicle characteristics that were assumed to be constant during the trajectory are given in table III.

## RESULTS AND DISCUSSION

### Initial Conditions

For a successful separation, the normal load factor on the orbiter must be greater than that on the carrier vehicle. The normal loadings on both vehicles in the launch configuration are shown in figure 4 for the baseline conditions established in figure 3 and a given control setting. Above the line at which both vehicles have identical loadings ( $\Delta \bar{n} = 0$ ), the vehicles are initially separating, since the load factor on the orbiter is greater than that on the carrier vehicle. The initial separation criteria for the attitudes  $\alpha_c$  and  $\alpha_i$  are established by this loading diagram. These attitude criteria are necessary conditions but not complete conditions for separation, since horizontal and rotational effects are not included.

### Initial Separation Studies

The initial separation trajectories presented in figure 5 use the initial conditions of table III and figure 3. The vehicles begin their separation maneuver in straight and level equilibrium flight. The carrier vehicle is in a high-drag configuration with reverse thrust from inboard engines, idle thrust from outboard engines, spoilers deployed, and the elevator set at  $5.5^\circ$  to trim the mated configuration. The orbiter elevons are initially set at  $5^\circ$ . The initial vehicle attitudes are selected to achieve initial separation as given by figure 4 ( $\alpha_c = 5.5^\circ$ ,  $\alpha_i = 9^\circ$ ). The controls for both vehicles remain fixed. At the beginning of the simulation, the orbiter is released from the carrier vehicle, and the vehicles initially separate. Since the vehicles, with controls

fixed, are instantaneously out of trim after the orbiter is released, they begin to pitch toward each other. Collision occurs between 2 and 3 sec.

To correct this problem, an attitude-hold autopilot, represented by equation (1), was employed. When the baseline conditions were used as a starting point and the autopilot was utilized to command the controls, a safe separation did occur. Figure 6 is a time history for the active-control maneuver. The commanded angles of attack for the orbiter and carrier vehicle are  $14^\circ$  and  $2^\circ$ , respectively, and the commanded pitch rate is 0 deg/sec for both vehicles. The maximum control deflection rate for both vehicles is limited to 20 deg/sec, and control deflection range is limited to  $\pm 20^\circ$ . After the orbiter is released, the autopilot moves the controls so that each vehicle seeks  $\alpha_{com}$  and  $\dot{\theta}_{com}$ ; after approximately 3.5 sec, the orbiter is free of the carrier vehicle and the controls reach a steady condition. In this steady-state condition, there is an error between the actual and commanded  $\dot{\theta}$  and  $\alpha$ . At this point for the carrier vehicle,  $\dot{\theta}$  is  $-0.61$  deg/sec and  $\alpha$  is  $4.03^\circ$ . With autopilot gains  $K_1$  and  $K_2$  equal to 20 and 6, respectively, the resulting  $\delta_e$  from equation (1) is equal to  $0^\circ$ . The gains were varied in an attempt to achieve greater accuracy, with little success. Even a more sophisticated control system could not eliminate this error, because the vehicles are not in an equilibrium glide condition. The simple control system represented by equation (1) was able to control the vehicles sufficiently to achieve separation and is used in the following analysis.

#### Preseparation Maneuver

Although successful separation of the orbiter from the carrier vehicle has been shown, this separation trajectory occurs only for one set of initial conditions. Before the orbiter is released from the carrier vehicle, a series of preseparation events must occur to ensure safe separation. A typical separation maneuver was simulated to determine its effect on initial conditions. Figure 7 is an illustration of this trajectory. The mated vehicles are initially flying straight and level with  $\alpha_i$  equal to  $9^\circ$ . For positive horizontal separation, the drag force on the carrier vehicle must be greater than that of the orbiter. Therefore at 14 sec before launch, the inboard engines of the carrier vehicle are put in reverse thrust and the outboard engines are throttled to idle thrust. To ensure initial vertical separation, the carrier-vehicle spoilers are deployed 4 sec later to increase  $\Delta \bar{n}$  by decreasing carrier-vehicle lift. An arbitrary delay of 8 sec is assumed before the orbiter is released in order to allow the flow about the vehicles to stabilize. The orbiter is then released and moves free of the carrier vehicle with the aid of active controls. At the time of launch, Mach number, altitude, and flight-path angle have varied from the conditions of straight and level flight which existed before the preseparation events were initiated.

#### Effect of Flight-Path Angle and Dynamic Pressure

The flight-path angle has a negligible effect on the separation trajectory as shown in figure 8 which illustrates just the separation displacement of the orbiter center of gravity relative to the center of gravity of the carrier vehi-



cle. The boundary in figure 8 represents a 1.75-m minimum clearance between the orbiter and the carrier vehicle. The variation in vehicle trajectory for different initial values of flight-path angle ( $\gamma = 0^\circ$  and  $-16^\circ$ ) is due to the effect of gravity. The gravitational acceleration of the vehicles in a dive ( $\gamma = -16^\circ$ ) increases the velocity of the vehicles, thus increasing the dynamic pressure. Because the time between the launch and the orbiter clearing the tail of the carrier vehicle is small ( $\approx 3$  sec), there is little velocity increase due to gravity.

In the present analysis, compressibility effects are neglected, since the proximity data were available only at Mach 0.20. Therefore, the effects of Mach number and altitude on the separation trajectory were related by an examination of the effects of dynamic pressure. The effect of changing the dynamic pressure by  $\pm 20$  percent from the nominal condition is shown in figure 9. The separation trajectory is nearly the same for each case, but the rate of separation varies directly with dynamic pressure.

### Horizontal Separation

To increase the horizontal separation of the vehicles, either the drag of the carrier vehicle must be increased or the drag of the orbiter must be decreased. Since the drag on the orbiter with a tail fairing cannot be significantly reduced, the effect of increasing horizontal separation by increasing carrier-vehicle drag was investigated by using various thrust schemes and by retracting or deploying the landing gear. To determine the effect of various devices that increase carrier-vehicle drag, a horizontal separation distance  $d$  is defined in figure 10 as the clearance between the carrier-vehicle tail and the orbiter tail fairing, measured with the orbiter level with the top of the carrier-vehicle tail. As shown in figure 10, maximum separation distance was accomplished with inboard engines in reverse thrust (137 000 N), outboard engines in idle thrust (36 000 N), and landing gear deployed. The spoilers produce only a small increase in drag; however, they have a significant effect on vertical separation as a result of the reduction in carrier-vehicle lift. (See table II.)

### Separation Envelope

A potential launch envelope based on the results from the separation analysis is illustrated in figure 11. The envelope is constructed with three boundaries. The separation boundary is developed from the fact that the orbiter will separate from the carrier vehicle if  $\Delta \bar{n}$  is greater than zero, when active controls are assumed to be used on both vehicles and the carrier vehicle is assumed to be in a high-drag configuration. The thrust-limit boundary represents the maximum  $\alpha_i$  for which the carrier-vehicle thrust can maintain straight and level flight at the given Mach number, altitude, and weight condition (thrust limit). The final boundary is the minimum design load factor that Lockheed-Georgia Company placed on the mated configuration, based on structural considerations. This launch envelope encloses a range of vehicle attitudes for which a successful separation can occur; thus, there is some flexibility in the pre-launch and launch maneuvers.

## CONCLUSIONS

A study has been conducted to determine the feasibility of separating the space shuttle orbiter from a large transport carrier vehicle at subsonic speeds. The longitudinal equations of motion for both vehicles were integrated by a digital computer program using interference aerodynamic data to determine separation feasibility. From this study, the following conclusions have been made:

1. Based on the available aerodynamic data, separation of the orbiter from a carrier vehicle is feasible for various dynamic-pressure and flight-path-angle conditions.

2. Both flight-path angle and dynamic pressure have negligible effects on the separation trajectory, but dynamic pressure has a direct relationship on the rate of separation.

3. To ensure safe separation, active controls are required to hold vehicle attitudes during separation.

4. The largest horizontal separation distance resulted with carrier-vehicle inboard engines in reverse thrust, outboard engines in idle thrust, and spoilers and landing gear deployed.

Langley Research Center  
National Aeronautics and Space Administration  
Hampton, VA 23665  
April 28, 1977

## REFERENCES

1. Decker, John P.; and Gera, Joseph: An Exploratory Study of Parallel-Stage Separation of Reusable Launch Vehicles. NASA TN D-4765, 1968.
2. Miller, C. W.; Higham, S. D.; Lineberger, L. B.; and Paterson, J. H.: C-5/Orbiter Piggyback Study - Volumes 1 and 2. Final Report LG74ER0051, Lockheed-Georgia Co., Apr. 1974.
3. Nichols, M. E.: Results of Investigations on an 0.015-Scale Configuration 140A/B Space Shuttle Vehicle Orbiter Model (49-0) in the NASA/Langley Research Center 8-Foot Transonic Pressure Tunnel (0A25). NASA CR-134,082, 1974.
4. Orlik-Rückemann, K. J.; and LaBerge, J. G.: Dynamic Interference Effect on Dynamic Stability of Delta-Wing Shuttle in Abort Separation at  $M=2.0$ . Lab. Tech. Rep. LTR-UA-18, Natl. Res. Counc. of Canada, Nov. 1971.

TABLE I.- ORBITER INCIDENCE ANGLES AND RELATIVE POSITIONS  
AT WHICH AERODYNAMIC DATA WERE OBTAINED

$\Delta Z/t_c$	$\alpha_i$ at $\Delta X/t_c$ of -	
	0.0	0.04
0.13	0.5, 5.5, 7.5, 10.0	0.5, 5.5, 10.0
.19	0.5, 5.5, 10.0	0.5, 5.5, 10.0
.25	0.5, 5.5, 10.0	0.5, 5.5, 7.5, 10.0

TABLE II.- CONTROL EFFECTIVENESS

Control surface	Interference free		Proximity	
	$C_{L\delta}$	$C_{m\delta}$	$C_{L\delta}$	$C_{m\delta}$
Orbiter elevon	0.021	-0.011	0.021	-0.011
C-5 elevator	.006	-.027	.005	-.022
C-5 horizontal tail	.008	-.032	.007	-.033
C-5 spoilers	-.011	.002	-.012	.003

TABLE III.- TRAJECTORY CONSTANTS

Aerodynamic parameters and vehicle characteristics	Carrier vehicle	Orbiter	Combination
$S, m^2$ . . . . .	576.0	249.9	576.0
$m, kg$ . . . . .	247 200	70 300	317 500
$I_Y, kg-m^2$ . . . . .	$37.22 \times 10^6$	$6.87 \times 10^6$	$45.42 \times 10^6$
$X_{cg}$ . . . . .	$0.222\bar{c}_c$	$0.65l_o$	$0.340\bar{c}_c$
$Z_{cg}, WL, m$ . . . . .	5.9	15.8	8.1
$C_{m\dot{\theta}}, rad^{-1}$ . . . . .	-32	-2	-32
$\bar{c}, m$ . . . . .	9.2	12.1	9.2
$l_c, m$ . . . . .	76.2		76.2
$l_o, m$ . . . . .		32.9	

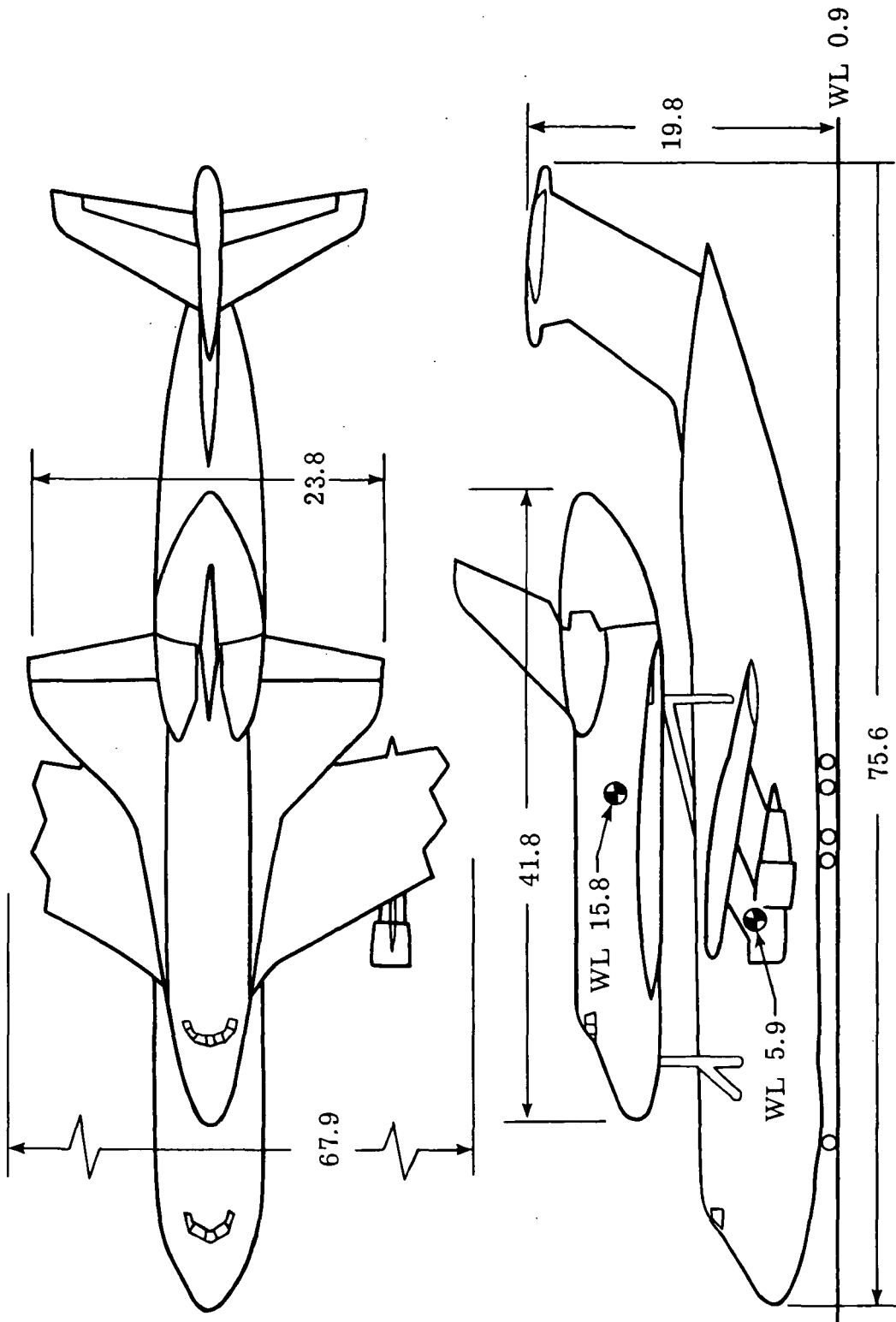


Figure 1.- Mated configuration. Dimensions are in meters.

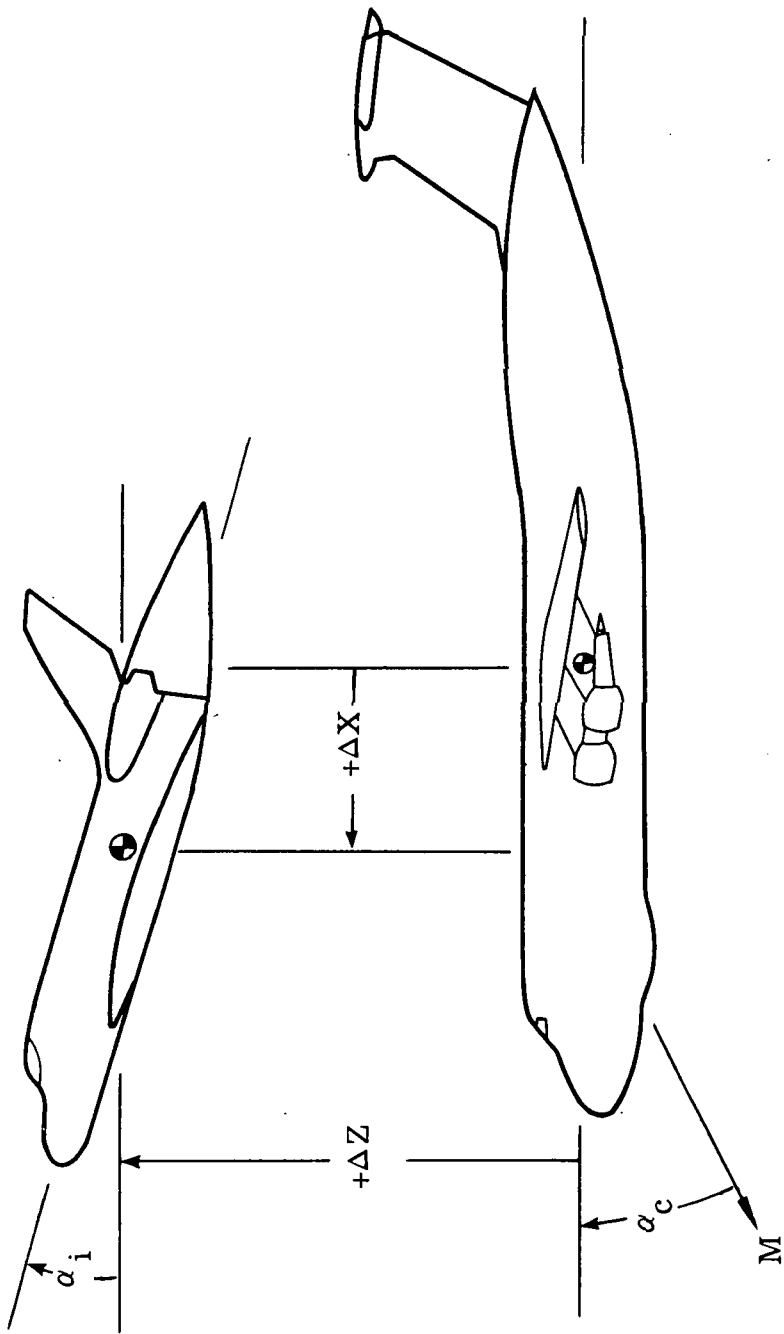


Figure 2.- Separation parameters.

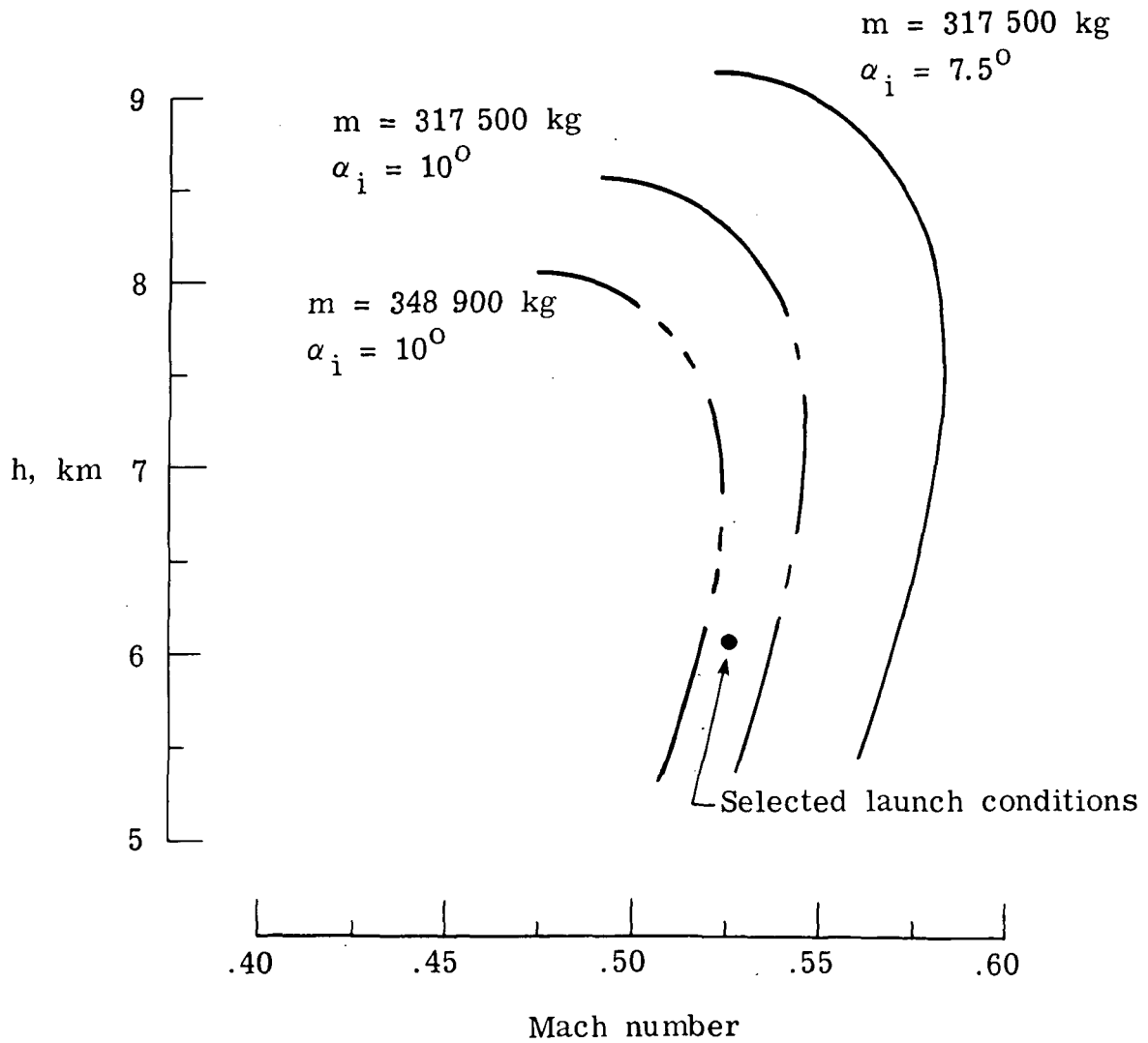


Figure 3.- Mated-vehicle flight envelope.

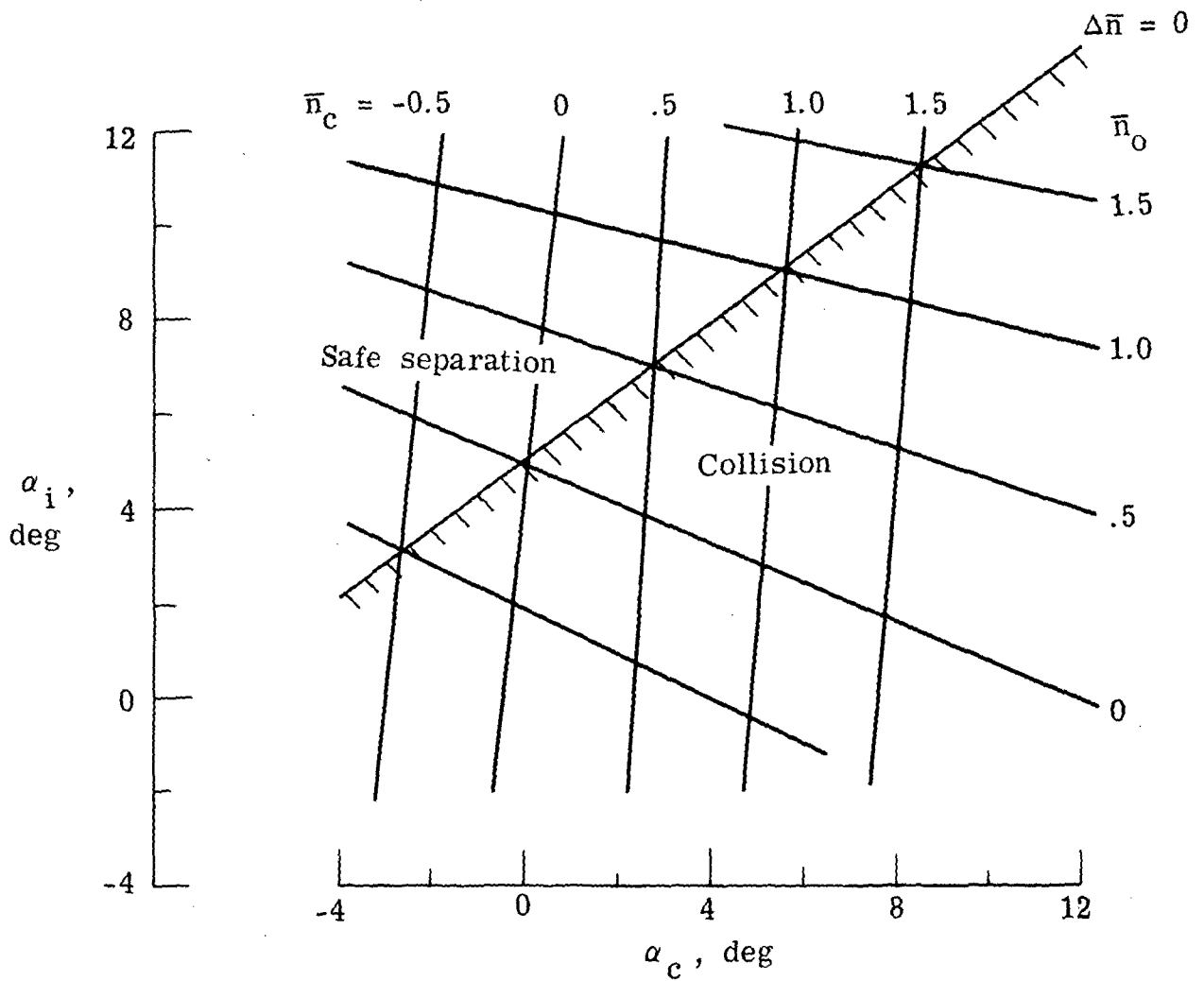


Figure 4.- Normal load factor diagram defining initial launch attitudes.  
 Initial launch conditions:  $m_c = 247\ 200$  kg;  $m_o = 70\ 300$  kg;  
 $h = 6.1$  km;  $M = 0.525$ ; carrier vehicle  $\delta_e = 0^\circ$  and spoilers up.



Fixed controls



Collision at  $t = 2.3 \text{ sec}$

Active controls



$t = 0 \text{ sec}$

$t = 3 \text{ sec}$

$t = 6 \text{ sec}$

Figure 5.- Initial separation studies showing effect of active controls. Initial launch conditions:  $m_c = 247 \text{ 200 kg}$ ;  $m_o = 70 \text{ 300 kg}$ ;  $h = 6.1 \text{ km}$ ;  $M = 0.525$ ; and high-drag carrier configuration.

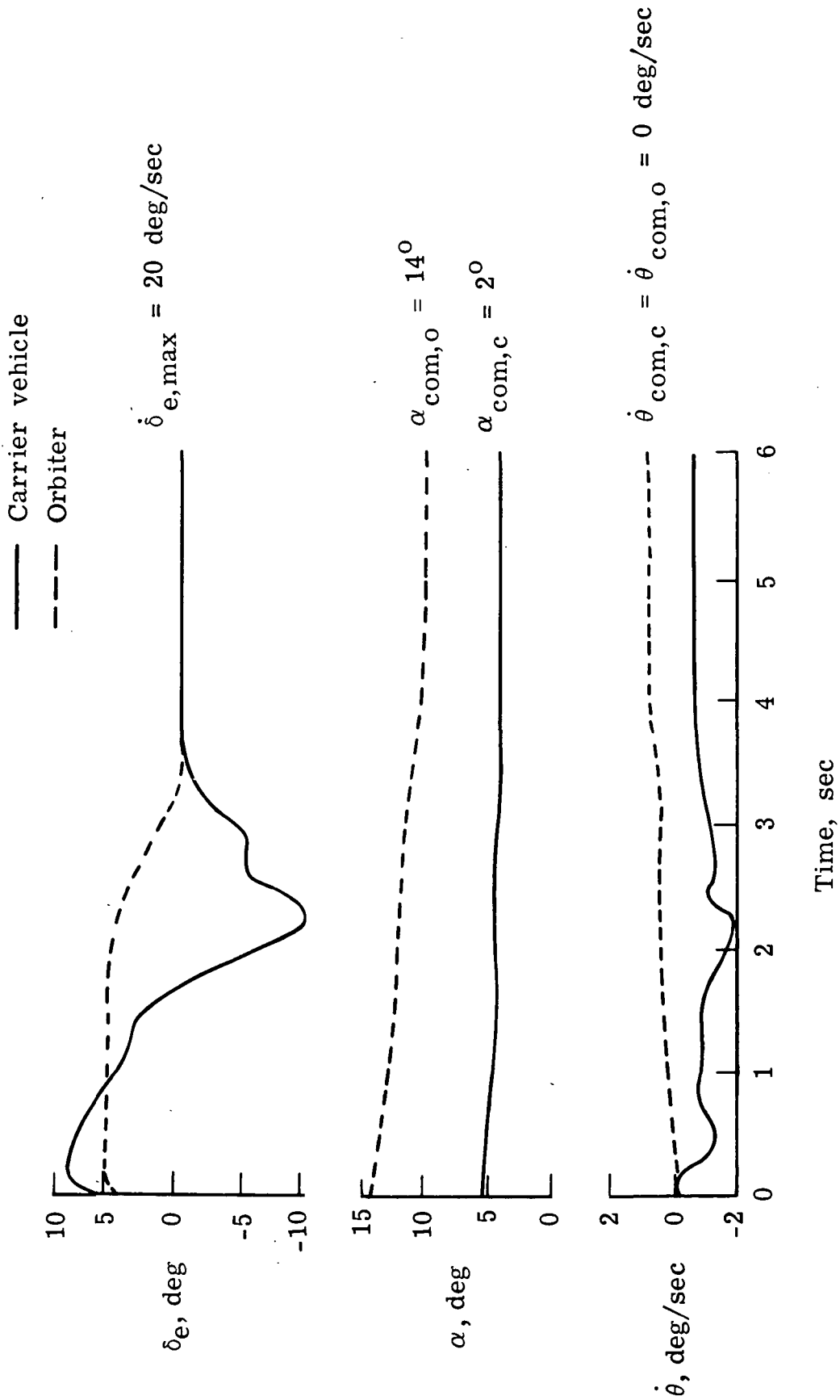


Figure 6.- Autopilot control history.

Thrust procedures initiated:

Reverse thrust - inboard engines

Idle thrust - outboard engines

Deploy spoilers

Delay to stabilize flow

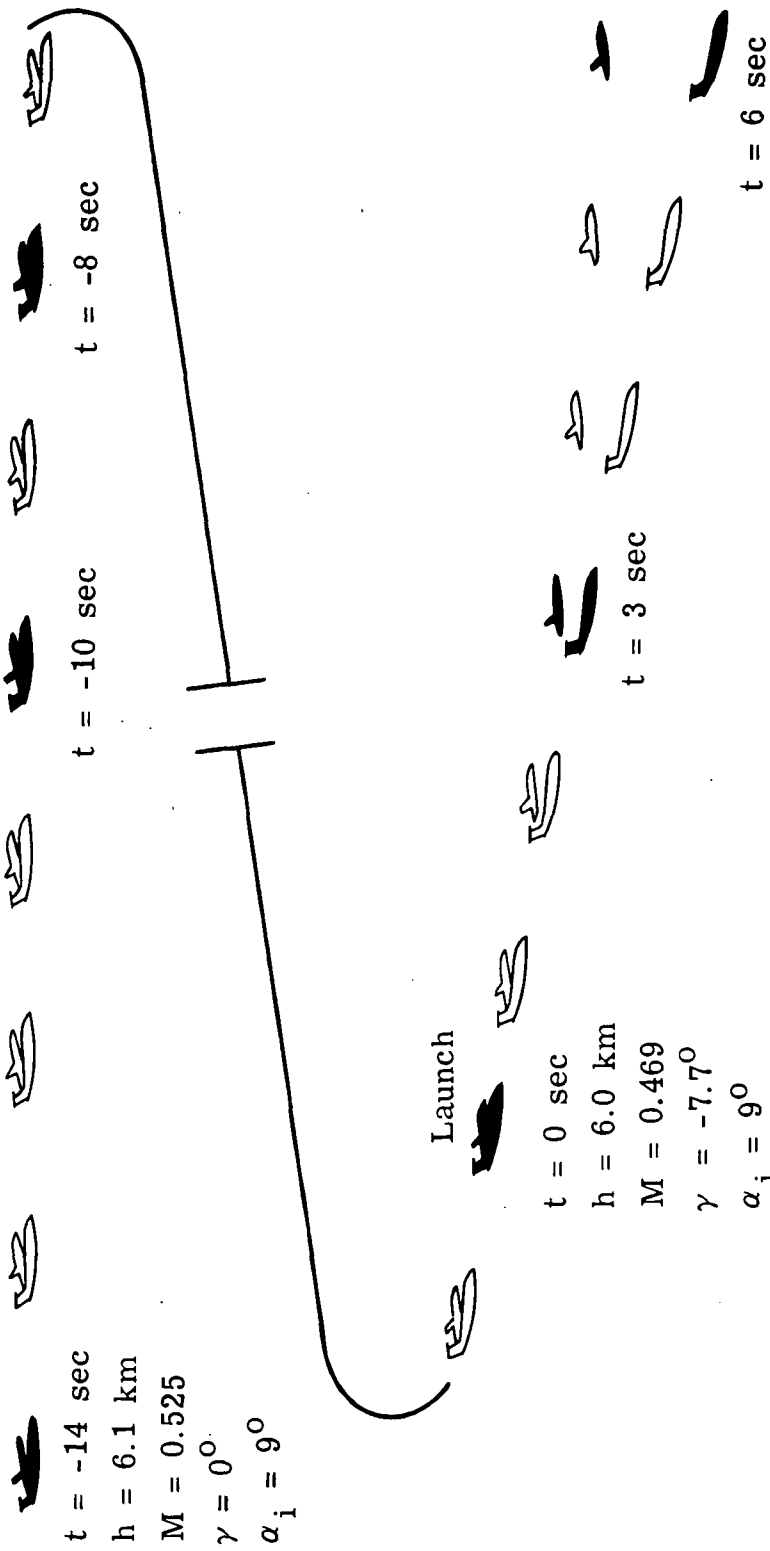


Figure 7.- Launch maneuver sequence. Launch conditions:  $m_c = 247 \text{ 200 kg}$  and  $m_o = 70 \text{ 300 kg}$ .

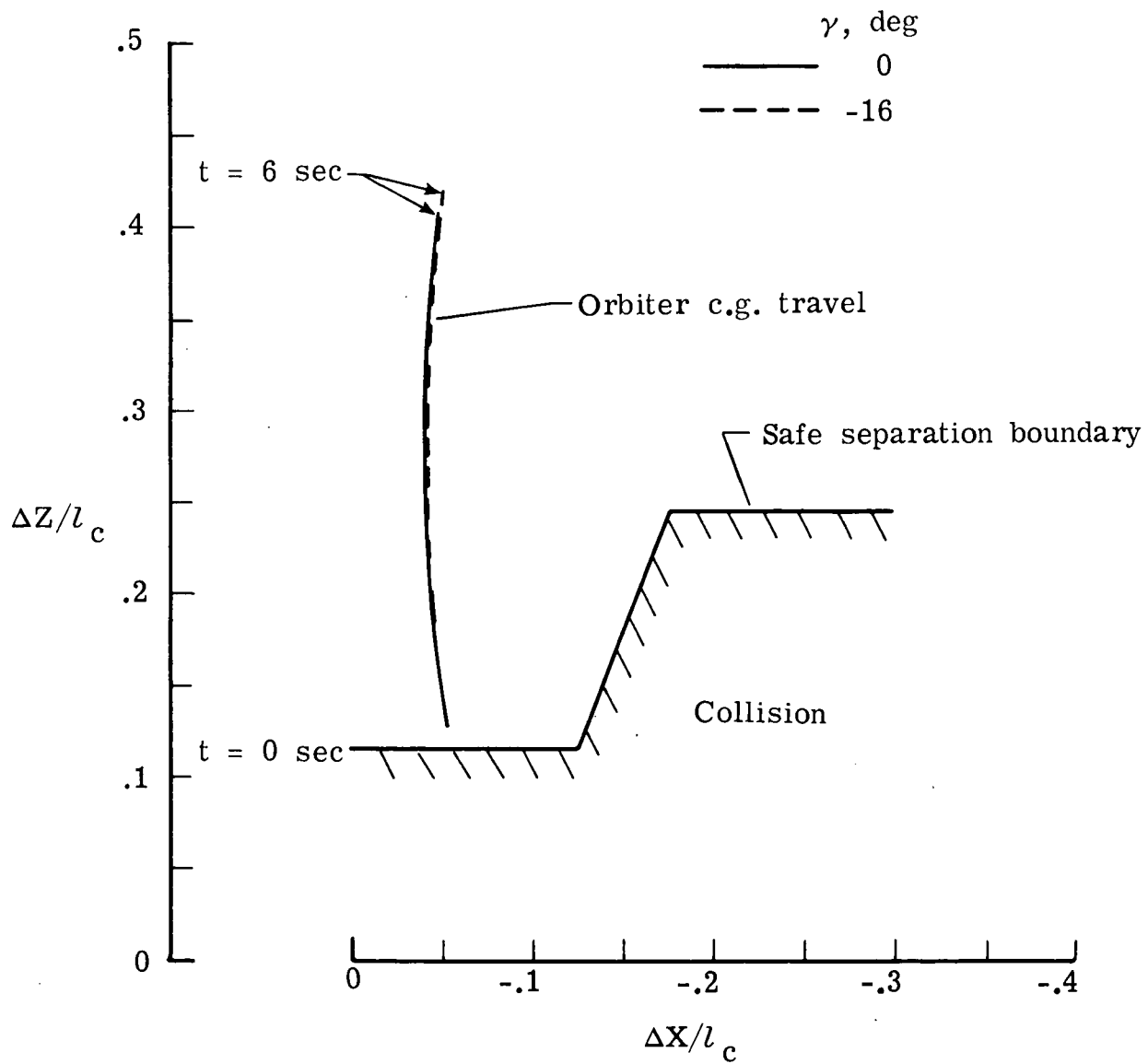


Figure 8.- Effect of flight-path angle on separation trajectory.

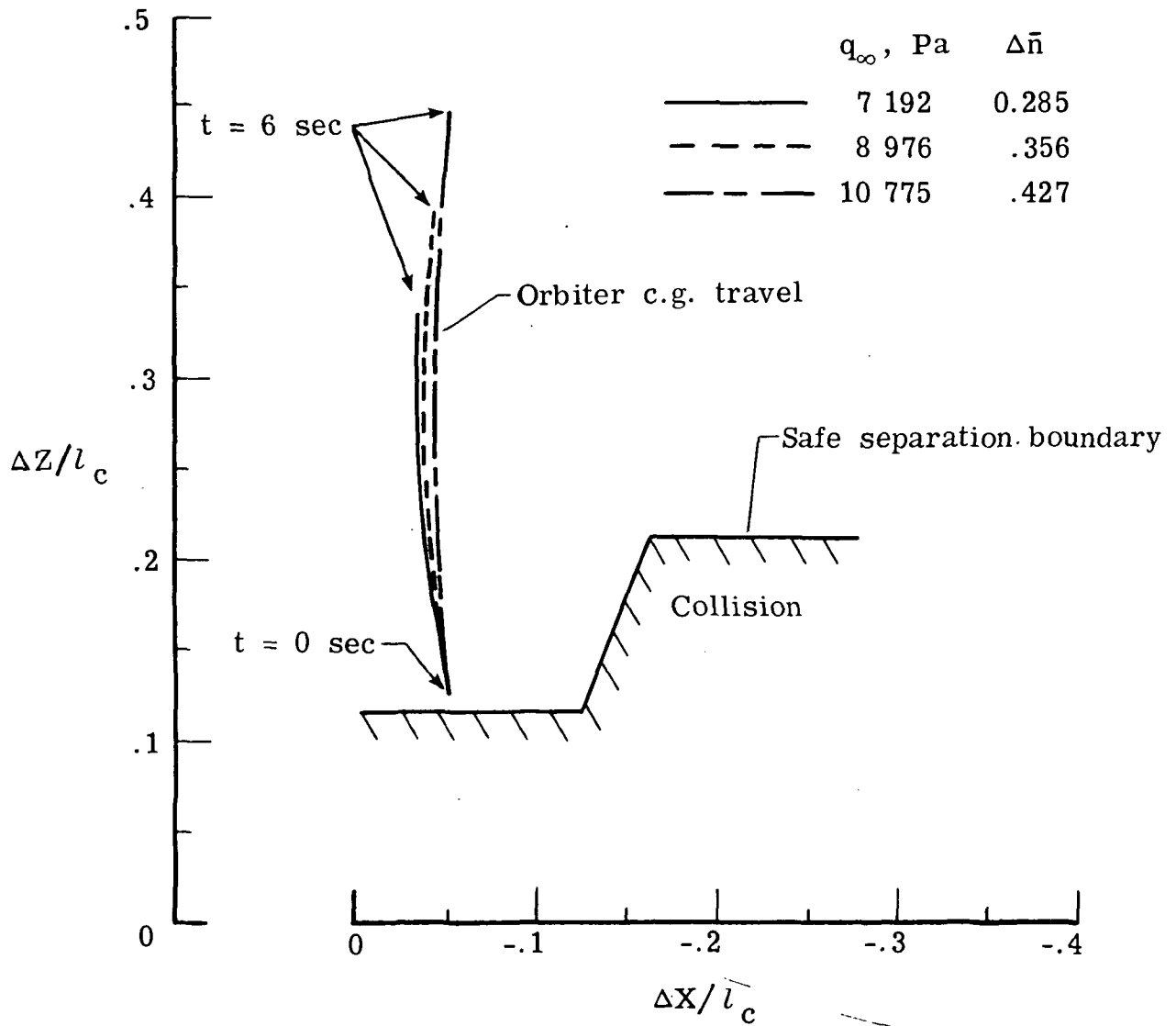
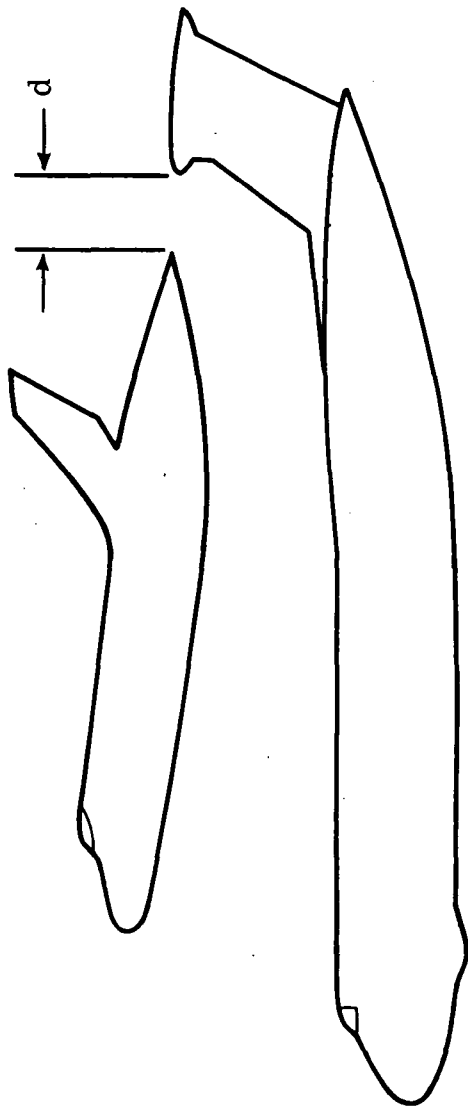


Figure 9.- Effect of dynamic pressure on separation trajectory.



<u>Thrust - inboard engines</u>	<u>Thrust - outboard engines</u>	<u>Spoilers</u>	<u>Landing gear</u>	<u>≈ d, m</u>
0	0	Deployed	Up	8.0
Idle	Idle	Deployed	Up	8.4
Reverse	Idle	Deployed	Up	9.6
Reverse	Idle	Deployed	Down	11.0

Figure 10.- Variation of horizontal separation distance. Launch conditions:  $m_c = 247\ 200\ \text{kg}$ ;  
 $m_o = 70\ 300\ \text{kg}$ ;  $h = 6.1\ \text{km}$ ; and  $M = 0.525$ .

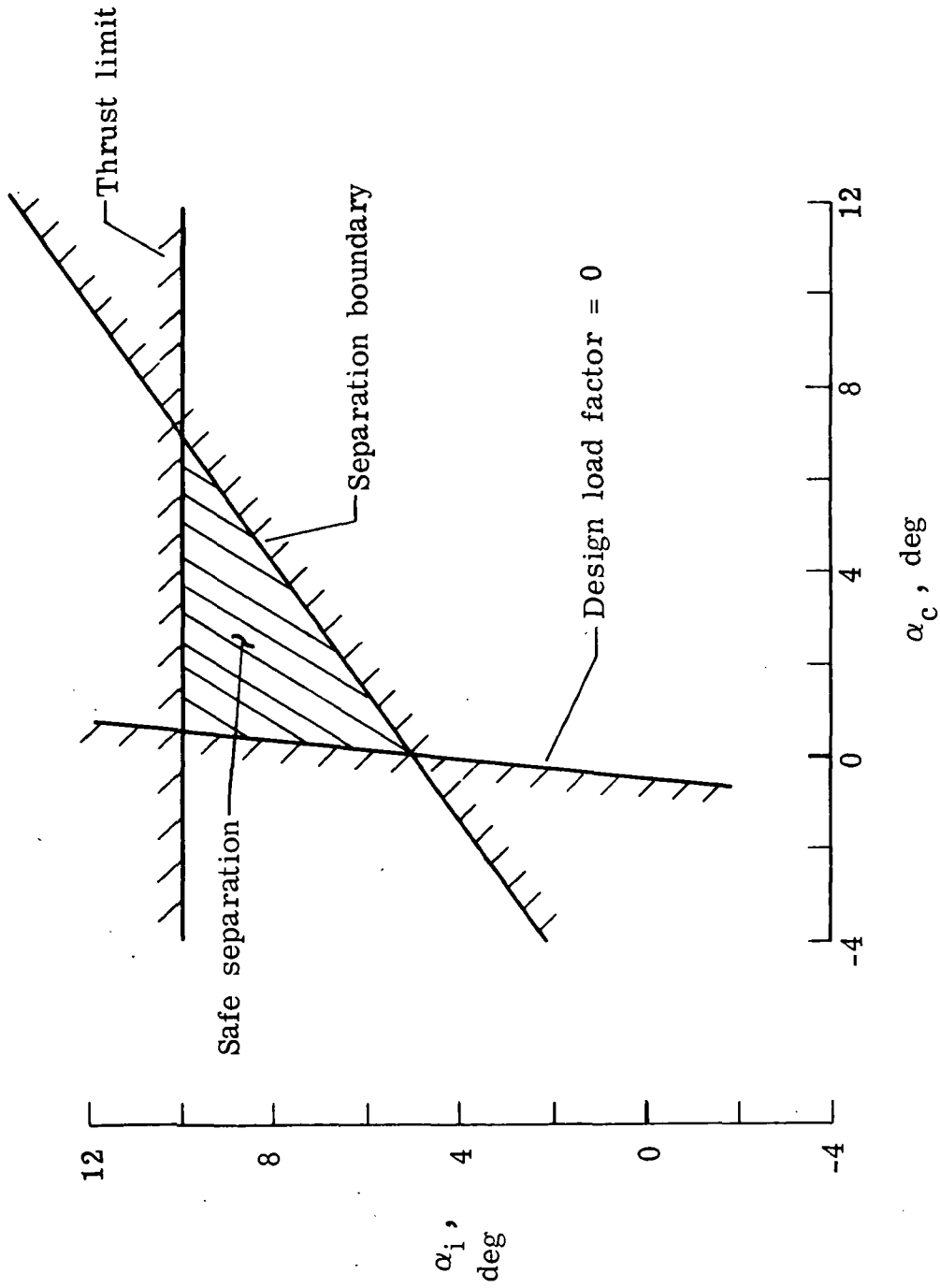


Figure 11.- Potential launch envelope for safe separation. Initial launch conditions:  $m_c = 247\ 200$  kg;  $m_o = 70\ 300$  kg;  $h = 6.1$  km; and  $M = 0.525$ .



POSTMASTER: If Undeliverable (Section 158  
Postal Manual) Do Not Return

*"The aeronautical and space activities of the United States shall be conducted so as to contribute . . . to the expansion of human knowledge of phenomena in the atmosphere and space. The Administration shall provide for the widest practicable and appropriate dissemination of information concerning its activities and the results thereof."*

—NATIONAL AERONAUTICS AND SPACE ACT OF 1958

## NASA SCIENTIFIC AND TECHNICAL PUBLICATIONS

**TECHNICAL REPORTS:** Scientific and technical information considered important, complete, and a lasting contribution to existing knowledge.

**TECHNICAL NOTES:** Information less broad in scope but nevertheless of importance as a contribution to existing knowledge.

**TECHNICAL MEMORANDUMS:** Information receiving limited distribution because of preliminary data, security classification, or other reasons. Also includes conference proceedings with either limited or unlimited distribution.

**CONTRACTOR REPORTS:** Scientific and technical information generated under a NASA contract or grant and considered an important contribution to existing knowledge.

**TECHNICAL TRANSLATIONS:** Information published in a foreign language considered to merit NASA distribution in English.

**SPECIAL PUBLICATIONS:** Information derived from or of value to NASA activities. Publications include final reports of major projects, monographs, data compilations, handbooks, sourcebooks, and special bibliographies.

**TECHNOLOGY UTILIZATION PUBLICATIONS:** Information on technology used by NASA that may be of particular interest in commercial and other non-aerospace applications. Publications include Tech Briefs, Technology Utilization Reports and Technology Surveys.

Details on the availability of these publications may be obtained from:

**SCIENTIFIC AND TECHNICAL INFORMATION OFFICE**

**NATIONAL AERONAUTICS AND SPACE ADMINISTRATION**

Washington, D.C. 20546